

# HASIL CEK\_Highly energy-efficient combination of dehydrogenation of methylcyclohexane and hydrogen-based power generation

*by* Zahrul Mufrodi 60010305

---

**Submission date:** 01-Nov-2021 09:52AM (UTC+0700)

**Submission ID:** 1689515963

**File name:** ion\_of\_methylcyclohexane\_and\_hydrogen-based\_power\_generation.pdf (1,000.95K)

**Word count:** 7287

**Character count:** 38184



# Highly energy-efficient combination of dehydrogenation of methylcyclohexane and hydrogen-based power generation

Firman Bagja Juangsa<sup>a, \*</sup>, Lukman Adi Prananto<sup>b</sup>, Zahrul Mufrodi<sup>c</sup>, Arief Budiman<sup>d</sup>, Takuya Oda<sup>b</sup>, Muhammad Aziz<sup>b, \*</sup>

<sup>a</sup> Department of Mechanical Engineering, Tokyo Institute of Technology, 2-12-1 Ookayama, Meguro-ku, 152-8550, Japan

<sup>b</sup> Institute of Innovative Research, Tokyo Institute of Technology, 2-12-1 Ookayama, Meguro-ku, 152-8550, Japan

<sup>c</sup> Chemical Engineering Department, Ahmad Dahlan University, Jl. Kapas 9, Yogyakarta 55166, Indonesia

<sup>d</sup> Chemical Engineering Department, Gadjah Mada University, Jl. Grafika 2, Yogyakarta 55284, Indonesia

## ARTICLE INFO

### Keywords:

Methylcyclohexane  
Dehydrogenation  
Hydrogen  
Graz  
Electricity  
Energy efficiency

## ABSTRACT

Hydrogen ( $H_2$ ) has been well studied for its potential use in energy storage, which is particularly related with the intermittent characteristic of renewable energy sources. However, the gas form of  $H_2$  at standard pressure and temperature (STP) poses a challenging problem in terms of storage, transportation, and low volumetric energy density. An effective and reversible method for  $H_2$  storage is chemically bonded  $H_2$  used in the toluene ( $C_7H_8$ )/methylcyclohexane (MCH,  $C_7H_{14}$ ) cycle. This study investigates a power generation system from  $H_2$  storage in MCH, involving the dehydrogenation process and the combined cycle as a power generation process. An adequate analysis of the heat circulation was performed through an enhanced process integration (EPI) to ensure the high energy-efficiency of the proposed system. A highly endothermic reaction of dehydrogenation was supplied by utilizing the energy/heat from air-fuel combustion to ensure the effective heat recovery of the system. The proposed system was analyzed through an adjustment of the main operating parameters, namely, the GT inlet pressure, GT inlet temperature, and the condenser pressure, to observe their effects on the efficiency of the system. It was found that these parameters have a significant influence on the system performance and provide the possibility of further improvement. Under optimum conditions, the proposed system can realize a very high system efficiency of 54.6%. Moreover, the proposed system is also compared to a Graz cycle-based system, which has been reported to achieve an excellent power generation cycle from  $H_2$ . This result implies that the proposed integrated system leads to a significantly higher power-generating efficiency. Numerically, the proposed system demonstrated a system efficiency of 53.7% under similar conditions as the Graz cycle based system, which achieved a system efficiency of 22.7%.

## 1. Introduction

Power generation from renewable energy sources has been studied for decades, and has been implemented at a large scale in many countries during recent years [1]. In addition, renewable energy is the fastest growing source of electricity generation, and it has been predicted that its share will increase to 39% by 2050 [2]. However, the power generation from renewable energy sources, particularly wind and solar, faces several challenges to a power grid operation, including an intermittent output and a mismatch between the power output and

demand, resulting in grid instability and wasted energy during a period of oversupply [3].

Electrical energy storage can be installed in the system to balance the energy between demand and supply, as well as store the surplus energy. Electrical energy storage in the form of chemical energy has been widely applied, such as through batteries, methane ( $CH_4$ ), and hydrogen ( $H_2$ ) [4]. Among such chemical storage types,  $H_2$  has the best ratio of valence electrons to protons, and therefore, the energy gain per electron is quite high [5]. Energy storage achieved by converting excess electricity into  $H_2$  through the water electrolysis (power-to-gas) process has been widely studied using well-established pilot plans [6,7]. In addition, the trends of decarbonization of fossil fuels and con-

\* Corresponding authors.

Email addresses: juangsa.f.aa@m.titech.ac.jp (F.B. Juangsa); aziz.m.aa@m.titech.ac.jp (M. Aziz)

version of biomasses into  $H_2$  have increased significantly owing to a high environmental concern and convenience [8,9]. The chemical energy per mass of  $H_2$  ( $142\text{ MJ kg}^{-1}$ ) is at least three-times higher than that of gasoline ( $44\text{ MJ kg}^{-1}$ ) [5,10]. Because  $H_2$  is one of the most abundant elements on Earth,  $H_2$  has a high potential as an energy storage or energy carrier, and it is believed that the role of  $H_2$  will increase in the future.

However,  $H_2$ , which is in gas form at standard pressure and temperature (STP), has been a challenging problem in terms of storage and transportation owing to its low volumetric energy density, which is only about  $3\text{ Wh L}^{-1}$  [11]. Therefore, an effective storage method of  $H_2$  will play a key role in  $H_2$  technology development. There are many types of  $H_2$  storage systems used with the general purpose of increasing the volumetric energy density of  $H_2$ . The compression of  $H_2$  is one of the basic technologies applied to increase the molecule density, resulting in an increase in the volumetric energy density [12]. High-pressure tanks are required with a rated pressure of 200–450 bar. However, high-pressure containers have several significant disadvantages in terms of an additional pressure control required during depressurization and the safety risk of  $H_2$  pressurization. Another method for  $H_2$  storage is liquefaction, which is condensing the gas into a liquid, or even a solid, because both phases have significantly higher density than the gaseous phase [5,13,14]. However, a very low condensation temperature ( $-252^\circ\text{C}$  at 1 bar) is required, and cryogenic technology consumes a large amount of energy, and there are still many challenging problems with regard to liquefaction, including super-insulated low-temperature storage methods [5,13].

Many studies related to the effective chemical storage of  $H_2$  have recently been conducted [15,16], including the use of organic materials and ammonia. Unfortunately, ammonia is poisonous and has a pungent odor [17]. The utilization of ammonia via combustion, such as gas turbine, has several problems including lower reactivity of ammonia and release of  $\text{NO}_x$ . Regarding the latter, the formation of  $\text{NO}_x$  increases significantly when the combustion temperature reaches about  $1500^\circ\text{C}$  following Zeldovich mechanism (thermal  $\text{NO}_x$ ). Therefore, as  $\text{NO}_x$  is a pollutant (GHG), direct utilization of ammonia via combustion is not environmental friendly. Although there are several technologies which can reduce the  $\text{NO}_x$  formation, however, they are still under development. In addition, in ammonia-based  $H_2$  chemical storage system,  $\text{N}_2$  is released during the dehydrogenation process, creating one-way transport from the site of  $H_2$  production to the site of  $H_2$  utilization. On the other hand, toluene in liquid phase as the result of dehydrogenation of MCH, will be returned to the hydrogenation plant and reused, allowing sustainable cycle of  $H_2$  storage system.

Chemical  $H_2$  storage can be applied by binding  $H_2$  to produce  $H_2$ -rich molecules in a catalytic hydrogenation reaction [15]. To create a sustainable  $H_2$  storage system, at least two processes, namely,  $H_2$ -rich molecule formation (hydrogenation) and  $H_2$  release (dehydrogenation), are required. Numerous molecules can be utilized in chemical storage, which can be distinguished into two main categories: (1) natural  $H_2$ -lean molecules that can be extracted from an exhaust gas mixture such as  $\text{CO}_2$  or  $\text{N}_2$ , and (2) a  $H_2$ -lean organic liquid, which allows a fully reversible cycle of hydrogenation/dehydrogenation. The latter is commonly referred to as liquid organic  $H_2$  storage (LOHC) [16,15].

LOHC technology has been widely studied, with an option of different organic material pairs such as methylcyclohexane (MCH,  $\text{C}_7\text{H}_{14}$ )-toluene ( $\text{C}_7\text{H}_8$ ), cyclohexane-benzene, decalin-naphthalene, and dibenzyl-toluene. Among the first three pairs, MCH-toluene is preferable for easier storage and transportation owing to its wide temperature range under a liquid state [18,19]. Among the available LOHCs, MCH-toluene and dibenzyl-toluene have a relatively high  $H_2$  content of 6.2% [20]. A dibenzyl-toluene pair has been recently reported with a focus on the dynamism of the system in supplying electricity [21]. However, this work remains at the laboratory scale, without a sufficient analysis at

larger scales, and is designed for fuel cell application. In contrast, the MCH-toluene cycle has been evaluated at the pilot scale by a Japanese company, and has been demonstrated to be effective [18]. Gaseous  $H_2$  is chemically bonded to toluene through hydrogenation forming liquid MCH [22]. Transportation and storage are the main features of MCH with a high boiling point, which make it a potentially safe medium for an  $H_2$  carrier. This is also very promising because up to 6–8 wt% of  $H_2$ , or 60–62  $\text{kg m}^{-3}$  (volume based under ambient conditions), can be stored [15,23]. Toluene as a raw material has been widely produced and utilized industrially, and provides a low-cost material for large-scale processes [23]. In addition, both toluene and MCH are in a liquid phase over a wide range of temperatures, which is favorable for long-term storage. At the industrial scale, in 2013, the Chiyoda Corporation began successfully operating a large-scale  $H_2$  storage and delivery system by utilizing toluene-MCH as an  $H_2$  carrier using a K-promoted  $\text{Pt}/\text{Al}_2\text{O}_3$  catalyst [18]. Therefore, the toluene-MCH cycle is theoretically promising as an  $H_2$  carrier, and is practically applicable at an industrial scale.

To gain energy from  $H_2$  bonded in MCH,  $H_2$  must be separated from toluene through a dehydrogenation process. The extracted  $H_2$  can be converted into electrical energy through thermal energy (a combined cycle) or chemical energy (a fuel cell). Numerous studies have been carried out to develop an efficient dehydrogenation process and electricity generation from MCH. Scherer et al. developed a seasonal electricity generation from MCH by employing solid oxide fuel cells (SOFCs) [24]. However, despite exhibiting high energy efficiency, SOFCs have very fragile characteristics owing to the reformation-based  $H_2$  used for the fuel [25]. Most studies on fuel cells have a common challenge in terms of the inability to provide a large power output [25,26]. It has been reported that, for power units with a capacity greater than 10 MW, steam-turbine-based units are preferable over fuel cell power units [27]. A hydrogen-fueled combustion turbine cycle (HFCTC) is expected to be a new energy source for the power sector, and certain countries, including Japan, have started its development [28]. To confirm its operability, a number of turbine manufacturers have reported studies on HFCTC, both numerically and experimentally, including  $H_2$ -fueled burners [28,29]. Milewski et al. investigated the utilization of  $H_2$  as a fuel based on a combined cycle concept with various plant utility configurations, and successfully achieved 60% energy efficiency [28]. Among these cycles, the Graz cycle has been developed further with an improved net efficiency of greater than 65% [26]. However, most of the combined cycles, including the Graz cycle, employ pure  $\text{O}_2$ , resulting in additional utilities and energy required for  $\text{O}_2$  separation from the air, leading to high-cost plants and a drop in efficiency of nearly 61% [26]. Moreover, the above studies have disregarded the hydrogenation process, and assumed that the  $H_2$  feed is in a pure phase, which is very difficult to achieve in a real operation. Regarding the large-scale production of MCH, Aziz et al. developed novel integrated concepts of large-scale MCH production from both low-rank coal [11] and brown coal [30] by applying chemical looping and hydrogenation using toluene. These concepts have achieved high values of  $H_2$  production while maintaining a clean technology for the environment. However, no evaluation regarding the dehydrogenation and utilization of  $H_2$  from MCH has been conducted.

To the best of the authors' knowledge, few investigations have addressed the concept of energy-efficient electricity production from  $H_2$  through MCH as a storage method. In this paper, we therefore propose the concept of an electricity generation plant, which is an integrated system consisting of dehydrogenation and combined cycle systems. The dehydrogenation of MCH is integrated with a combined hydro-fuel cycle, which employs ambient air for combustion. Therefore, the proposed system is more realistic as it is based on a comprehensive energy balance analysis of the cycle. An adequate analysis of the heat circula-

It has been conducted through enhanced process integration (EPI) to ensure the high energy-efficiency of the proposed system.

## 2. Process modeling

### 2.1. Conceptual model

The proposed integrated-system was designed and optimized based on the principles of EPI in order to significantly reduce the exergy loss throughout the integrated system. EPI focuses mainly on the heat circulation optimization throughout the systems by promoting an effective exergy recovery and process integration, leading to minimum exergy loss [31]. Exergy recovery is initially performed in each single process in order to achieve the optimum heat recovery through an exergy rate elevation and heat coupling [32]. In addition, the unrecoverable heat from any process is utilized further in other processes. Therefore, the unrecoverable heat can be minimized, resulting in minimum energy waste into the environment, and a high energy-efficiency of the system. Such technology has been applied to several processes, including drying [33],  $H_2$  production from algae [34], and biomass gasification [35].

Fig. 1 shows a conceptual diagram of the proposed integrated system. The system consists of three combined modules: MCH dehydrogenation,  $H_2$  combustion, and a combined cycle power generation. The solid, dotted, and dashed lines represent the material, heat, and electric flows, respectively.

One of the main processes of the systems is the highly endothermic dehydrogenation reaction of MCH, which contains a 6.2wt% capacity of  $H_2$ . MCH is supplied and transported from the hydrogenation plant using a large-sized vessel or pipeline. A packed bed reactor is employed in this module, and equipped with a catalyst to improve the reaction. Thermal energy for a dehydrogenation reaction is supplied mainly from recovered heat through pre-heating and combustion module exhaust before its remaining heat is converted into electrical energy through a combined cycle module.

As the main product of the dehydrogenation module,  $H_2$  is further fed to the combustion module, whereas the separated toluene is returned to the hydrogenation plant for another cycle to be utilized as a carrier substance. In the combustion module,  $H_2$  as a fuel is reacted with  $O_2$  from the air, converting the chemical energy of  $H_2$  into thermal energy. To obtain a reasonable combustion temperature, particularly the designated gas turbine inlet temperature, gas and steam discharged from the combined cycle are supplied back to the combustion chamber, cooling the burners and liners, and also controlling the fuel gas temperature. Exhaust gas, consisting of high-pressure and high-temperature steam and gas, leaves the combustion chamber under a pre-determined temperature condition.

The last module, the combined cycle module, converts the thermal energy of the exhaust gas into electricity by utilizing the combination

of gas and steam turbines. The hot exhaust gas from combustion is utilized initially as a heat source for the packed bed reactor to conduct dehydrogenation through a heat exchanger immersed inside the reactor, and sequentially flows to the combined cycle module for expansion.

### 2.2. Detailed system

In this section, a detailed design of the system is explained based on the process flow diagram shown in Fig. 2. The proposed system was evaluated through a theoretical calculation and software modeling using Aspen HYSYS ver. 8.8 (Aspen Technology, Inc.). To establish the model of the system, the following additional assumptions were employed during the calculations:

- The rated flow rate of MCH is  $100 \text{ t h}^{-1}$ .
- Heat exchangers, including HRSG, are a counter-flow type.
- The ambient pressure and temperature are 101.33 kPa and  $25^\circ\text{C}$ , respectively.
- The kinetic and potential energy losses are negligible.
- Air consists of 79 mol%  $N_2$  and 21 mol%  $O_2$ .
- The adiabatic efficiency of the pump and compressor is 90%.
- The pressure drop in the heat exchanger is 2%.
- The minimum approach temperature in the heat exchanger is  $10^\circ\text{C}$ .
- There are no external heat losses.

#### 2.2.1. MCH dehydrogenation

The dehydrogenation module employs a packed bed reactor, and a catalyst is used inside the reactor to improve the following reaction. In addition, the pressure drop across the reactor is approximated using the following Eq. (2) [36]:

$$C_7H_{14} \rightarrow C_7H_8 + 3H_2 \quad \Delta H = 204.6 \text{ kJ mol}^{-1} \quad (1)$$

$$\Delta P = \frac{12.5(1 - \epsilon)^2}{\epsilon^3} \times (29.32Re^{-1} + 1.56Re^{-n} + 0.1) \frac{\rho u^2}{2} \frac{1}{d_p} \quad (2)$$

Among the various hydrogenation catalysts, a Pt catalyst has been studied by a number of researchers [22,37,38]. A theoretical review on the reaction kinetics and experimental results have shown that Pt/ $Al_2O_3$  is considered the best catalysts for MCH dehydrogenation in terms of activity, selectivity, and stability [22,38]. Dehydrogenation is an endothermic reaction, and therefore the required thermal energy is initially supplied through a self-heat exchange between the cold stream (process stream, F3) and hot stream (combustion flue gas, F9).

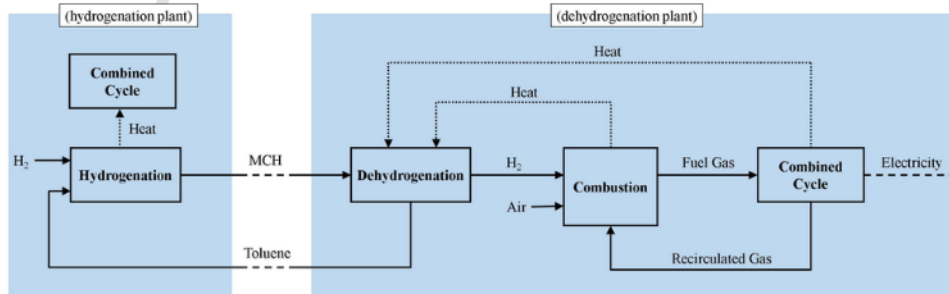


Fig. 1. Conceptual diagram of proposed integrated system.



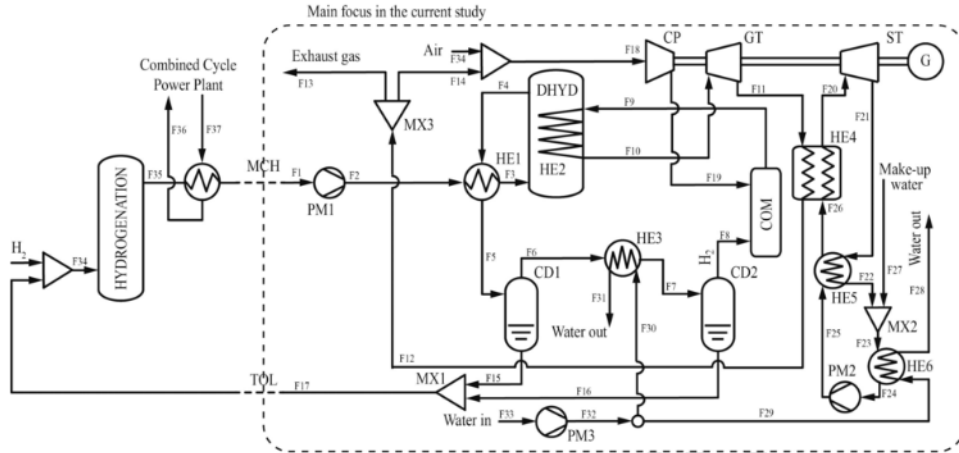
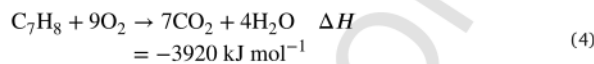
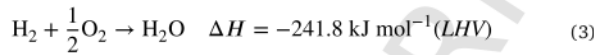


Fig. 2. Arrangement and process flow diagram of the proposed integrated system.

Toluene, as an  $H_2$  carrier, is returned to a hydrogenation plant (F17) for another cycle as an  $H_2$  storage system.

### 2.2.2. Combustion

$H_2$  produced from the dehydrogenation module is fed into the combustion chamber to be reacted with  $O_2$  included in the air, converting the chemical energy of  $H_2$  into thermal energy. Furthermore, thermal energy produced from a combustion reaction is utilized for producing the electricity in the combined cycle module, and the remaining heat is utilized to provide the thermal energy required for an endothermic reaction of dehydrogenation. Owing to the carbon-free combustion process of  $H_2$ , carbon dioxide ( $CO_2$ ), which well known to be the main contributor of greenhouse gasses, is not emitted, as shown in reaction (3). In this study, after dehydrogenation, the gas and liquid phase substance is separated into separators (CD1, CD2) and cooled through water cooling (F30). Owing to the extremely different boiling temperature,  $H_2$  is discharged in a gas phase, whereas toluene is discharged in a liquid phase. However, small portions of toluene in the gas phase remain and are mixed with  $H_2$ , flowing into the combustion chamber. Therefore, a very small amount of  $CO_2$  production may occur, as shown in reaction (4).



### 2.2.3. Combined cycle for electricity generation

The combined cycle consists of three main components: a gas turbine (GT), steam turbine (ST), and heat recovery steam generator (HRSG). EPI is applied throughout the system, including the heat circulation during the dehydrogenation, and the combined cycle to enhance the optimum heat circulation of the system and achieve a high energy-efficiency. Table 1 summarizes the conditions and assumptions for each module of the dehydrogenation and combined cycle.

In this study, the combined cycle is employed with a modification of the Graz cycle, whereas the exhaust gas from HRSG (F14) is partially returned to the combustion chamber for cooling, as well as to improve the energy density owing to the high heat capacity of water. Originally, the Graz cycle utilizes high-pressure steam from a high-pressure steam turbine to be fed into the combustion chamber for cooling [26,40].

Table 1  
Assumed conditions for each module of the dehydrogenation and combined cycle.

Parameter	Value	Symbol (Refer to Fig. 2)
<i>Dehydrogenation (DHYD)</i> [18,21,22,39]		
Reactor temperature ( $^{\circ}C$ )	450	F4
Internal pressure (kPa)	120–150	DHYD
Catalyst	Pt/ $Al_2O_3$	–
Fuel temperature before separation ( $^{\circ}C$ )	70	F7
Minimum toluene discharge ratio	90%	F17
<i>Power generation – Gas turbine (GT)</i> [11,26]		
Isentropic efficiency (%)	90	–
Inlet temperature ( $^{\circ}C$ )	1400–1600	F10
Inlet pressure (MPa)	2.8–4.0	F10
<i>Power generation – Steam turbine (ST)</i> [11,26]		
Isentropic efficiency (%)	90	–
Inlet pressure (MPa)	10	F20
Steam turbine inlet temperature ( $^{\circ}C$ )	522–581	F20
Minimum vapor quality	0.9	–

However, in this study, the gas exhausted from the HRSG outlet is used instead of high-pressure steam, leaving the steam expansion process in the ST for optimum electrical generation. The HRSG outlet gas also has a lower temperature, providing an effective cooling process in the combustion chamber.

## 3. Results and discussion

The performance of the proposed integrated system was evaluated through the optimization of several key operating parameters with regard to a detailed system performance, and the energy efficiency of the system was compared with other similar systems. The performance of the system was evaluated by determining the system efficiency ( $\eta_{\text{power}}$ ) as follows:

$$\eta_{\text{system}} = \frac{W_{\text{net}}}{(\dot{m}_{\text{MCH}} \times \text{LHV}_{\text{MCH}} - \dot{m}_{\text{Toluene}} \times \text{LHV}_{\text{Toluene}})} \quad (5)$$

where  $\dot{m}_{\text{MCH}}$ ,  $\dot{m}_{\text{Toluene}}$ ,  $\text{LHV}_{\text{MCH}}$ , and  $\text{LHV}_{\text{Toluene}}$  are the mass flow rate of MCH, mass flow rate of toluene, LHV of MCH, and LHV of toluene,

respectively. The generated net power as the final result of this system is compared with the difference in calorific value between MCH, as an input material, and toluene, as an output material. The net generated power ( $W_{net}$ ) is calculated based on the total power generated by the GT ( $W_{GT}$ ) and ST ( $W_{ST}$ ) with a consideration of the power consumed by auxiliaries ( $W_{Aux}$ ), which is shown as follows:

$$W_{net} = W_{GT} + W_{ST} - W_{Aux} \quad (6)$$

### 3.1. Detailed system performance

The effects of various operating conditions, including the GT inlet pressure, GT inlet temperature, and ST inlet pressure, on the overall power generation and its efficiency were considered in this study. Calculations using Aspen HYSYS were utilized to investigate the required objectives.

#### 3.1.1. GT inlet pressure

Fig. 3 shows the effects of the variations in GT inlet pressure on the system efficiency under different GT inlet temperatures. It has been shown that the system efficiency increases following an increase in GT inlet pressure. Numerically, the highest system efficiency, which is 54.6% (net generated power of 132MW), is achieved under a GT inlet pressure and temperature of 4MPa and 1600°C, respectively. This system efficiency decreases to 52.6% (net generated power of 128MW) when the GT inlet pressure is decreased to 2.8MPa under the same GT inlet temperature.

In detail, power generated by GT and ST increases at a higher pressure of the fuel gas owing to higher enthalpy. However, the power consumed by the compressor also increases, resulting in a compensation relationship between the GT inlet pressure and the compressor power consumption. At high temperature, the amount of additional power generated by a pressure increase is relatively higher than that achieved through an additional compressor application. However, at a lower temperature, the compressor operation increasing the gas pressure is higher than the total generated power, resulting in a decrease in the system efficiency. To decrease the GT inlet temperature, more recirculated gas (F14) is required, causing an increase in the gas flow rate, and leading to a higher compressor load. The GT inlet pressure, shown as F10 in Fig. 2, is determined based on the compression ratio of the compressor (CP). The influence of the compression ratio on the combined cycle performance has been reported well in other similar arrangements of the combined cycle [26,41]. The energy required for compression significantly affects the net power generated by the combined cycle module.

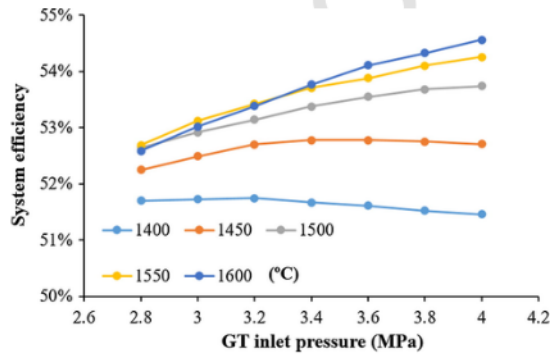


Fig. 3. System efficiency as a function of GT inlet pressure under different GT inlet temperatures.

#### 3.1.2. GT inlet temperature

Fig. 4 shows the influence of the GT inlet temperature on the system efficiency under different GT inlet pressures. In general, the GT inlet temperature strongly influences the system efficiency. At a GT inlet pressure of 4MPa, the system efficiency increases from 52.7% (net generated power of 127MW) to 54.6% (net generated power of 133MW) when the GT inlet temperature is increased from 1400°C to 1600°C.

The GT inlet temperature is determined through a combustion reaction, which produces a very high-temperature flue gas, and by the temperature of the recycled gas from the HRSG outlet. The system efficiency increases with a higher GT inlet temperature. A higher gas temperature has a higher exergy rate leading to larger energy/heat, which can be recovered by GT. Moreover, a higher GT inlet temperature results in less re-circulated gas, leading to a lower energy required for compression. However, as mentioned previously, the system performance is significantly influenced by the GT inlet pressure, which determines the amount of gas flow. A high GT inlet temperature causes a lower gas flow, affecting the amount of power generated by ST. The ST power is the compensation between the flue gas temperature and flow, as can be observed at a GT inlet pressure of 2.8MPa, where system efficiency decreases when the GT inlet temperature reaches above 1550°C.

#### 3.1.3. Condenser pressure

Another operating parameter that is believed to significantly influence the performance of the combined cycle is the condenser (HE6) pressure. Based on the thermodynamic curve, the condenser pressure, as the lowest pressure in the module, greatly affects the ST output. Fig. 5 shows the condenser pressure effect on the system efficiency at a GT inlet pressure and temperature of 4MPa and 1500°C, respectively. In general, the system efficiency increases following the lower pressure (more vacuum condition) of the condenser. The system efficiency increases from 53.7% to 52.9% when the condenser pressure is decreased from 85 to 35kPa.

The condenser temperature is directly affected by the pressure owing to the saturated condition in the condenser. The lower pressure in the condenser can provide a lower temperature of ST expansion, which based on a Carnot cycle improves the system performance [42].

#### 3.1.4. Optimum system condition

The optimum system condition is determined based on the main parameters, and was analyzed in the previous sections as resulting in the maximum system efficiency. Table 2 shows the mass flow rate, pressure, and temperature of the major flows, which represent the system performance under an optimal operation (GT inlet pressure of 4MPa, GT inlet temperature of 1600°C, and condenser pressure of 35kPa).

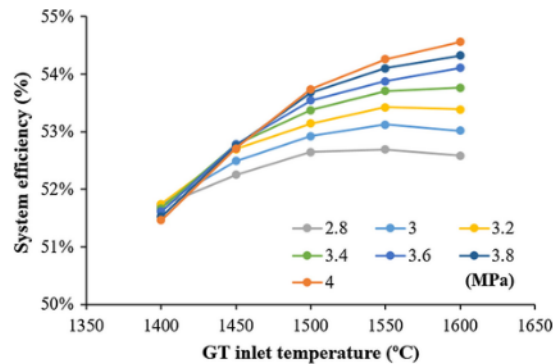


Fig. 4. System efficiency as a function of GT inlet temperature under different GT inlet pressures.

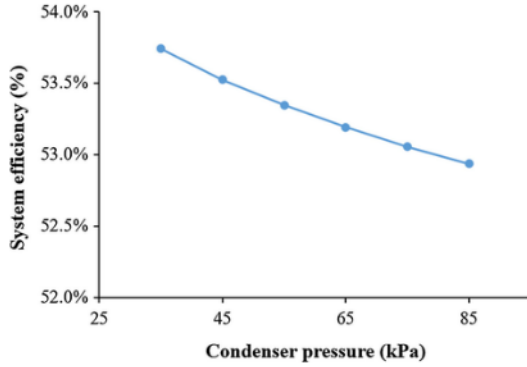


Fig. 5. System efficiency as a function of condenser pressure (GT inlet pressure and temperature of 4 MPa and 1500 °C, respectively).

### 3.2. Performance comparison with Graz cycle-based power generation

In terms of  $H_2$  utilization when using steam turbine cycles, a number of studies have been reported under various configurations [28]. However, they have focused particularly on power generation from  $H_2$ . In this study, we compared our proposed system with another system, including the dehydrogenation process in each system. The power generation efficiency, described in Eq. (5), was compared for each configuration because it represents the overall performance, including the dehydrogenation process.

Table 3 shows the main parameters and system performance of the proposed integrated system compared with the Graz cycle, which is integrated with the dehydrogenation process (Graz cycle-based system), for a comprehensive analysis. The dehydrogenation process in the Graz cycle-based system is calculated through a stoichiometric reaction shown in Eq. (1). The amount of MCH and toluene are calculated based on the  $H_2$  mass flow rate, with a toluene discharge ratio of 0.9. Although each system has a different rated power output, the system efficiency represents the overall system performance.

The Graz cycle employs oxy-fuel combustion, in which pure  $O_2$  is supplied from an air separation unit (ASU) and through the  $O_2$  compression process. Therefore, an additional power consumption of 24.3 MW is supplied from the generated power. Our proposed integrated system utilizes air-combustion, eliminating the requirement of ASU and an additional compression system. The power generation efficiency ( $\eta_{power}$ ) can be calculated for each system based on the following equation:

$$\eta_{power} = \frac{W_{net}}{(\dot{m}_{H_2} \times LHV_{H_2})} \quad (7)$$

Table 2

Conditions of major flows under optimum operation (GT inlet pressure of 4 MPa, GT inlet temperature of 1600 °C, and condenser pressure of 35 kPa).

Stream	Flow (t h <sup>-1</sup> )	Pressure (kPa)	Temperature (°C)	Stream	Flow (t h <sup>-1</sup> )	Pressure (kPa)	Temperature (°C)
F1	100	101.3	25	F11	597	150	710
F2	100	152	25	F12	597	147	80
F3	100	149	368	F17	85.3	140	37
F4	100	146	450	F19	597	4040	632
F5	100	143	70	F20	157	20,000	550
F7	78	140	25	F21	157	35	73
F8	14.7	140	25	F24	157	34	40
F9	597	4040	1845	F25	157	20,050	41
F10	597	4000	1600	F26	157	20,030	65

where  $W_{net}$ ,  $\dot{m}_{H_2}$ , and  $LHV_{H_2}$  are the net power generation, mass flow rate of  $H_2$ , and LHV of  $H_2$ , respectively.

Compared to the Graz cycle-based system (with a power generation efficiency of 60.37%), as shown in Table 3, the integrated system proposed in this study shows a higher power generation efficiency of 63.7%. This may indicate that an air-fuel combustion cycle is more efficient than an oxy-fuel combustion cycle in terms of the total energy efficiency owing to the excessive power consumption of ASU. Furthermore, Sanz et al. proposed the use of the Graz cycle as an efficient power generation under the assumption that high purity  $O_2$  is available as a by-product from the  $H_2$  production through electrolysis [26]. Therefore, in an integrated  $H_2$  storage and power generation system, in which  $O_2$  is unavailable within the process, as proposed in the present study, air-fuel combustion is considered to be more effective. In addition, air-fuel combustion has been well applied in a typical combined cycle plant with fewer components, providing a low initial power plant cost.

In this study, an integrated power generation system achieved through  $H_2$  storage (MCH) is proposed. The overall system performance was analyzed by comparing the system efficiency ( $\eta_{system}$ ) for both a Graz cycle-based system and the proposed integrated system. The dehydrogenation process in the Graz cycle-based system was calculated stoichiometrically based on the reaction shown in Eq. (1). Moreover, the energy required for the endothermic reaction of dehydrogenation was calculated under the assumption that the dehydrogenation system was designed based on conventional heat recovery technology for minimum exergy loss.

The proposed integrated system was shown to have a significantly higher efficiency of 53.7% compared to the Graz cycle-based system, at 23%. The system efficiency of the Graz cycle-based system is lower due to an extensive energy demand following an endothermic reaction of dehydrogenation. In addition, in the proposed integrated-system, the hot flue gas after combustion (F9) has a higher temperature (1722 °C) than that of the Graz cycle-based system (1500 °C). High-temperature gas is used as the thermal energy source for a reaction, reducing the exergy loss from the system, and thereby increasing the overall system efficiency.

In addition, further improvement can be achieved in the proposed system by decreasing the condenser pressure. As shown in Fig. 5, the system efficiency increases at a lower condenser pressure. The condenser pressure of the proposed integrated system is set to 35 kPa, although it can be decreased further to as low as that of the Graz cycle-based system (2.5 kPa). With a lower condenser pressure, it is expected that the proposed integrated system can achieve higher power generation efficiency, and thus higher system efficiency.

**Table 3**

Comparison of the main parameters and integrated system performance of Graz cycle based system [26] and the proposed integrated-system.

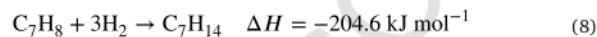
	Graz cycle-based system [26]	Proposed integrated system	Unit
<i>Conditions</i>			
Combustor outlet temperature	1500	1722	°C
GT inlet temperature	1500	1500	°C
GT inlet pressure	4	4	MPa
ST inlet pressure	17	20	MPa
Condenser pressure	0.0025	0.035	MPa
Minimum steam quality	0.893	0.9	
<i>Power Generation</i>			
GT power output	231.8	235.4	MW
ST power output	52.2	41.7	MW
Auxiliary power (pumps, etc.)	78.6	146.4	MW
ASU + O <sub>2</sub> compression	24.3	– <sup>a</sup>	MW
Net power	205.4	130.7	MW
Hydrogen LHV	120	120	MJ/kg
Hydrogen mass flow	2.5	1.71	kg/s
Power generation efficiency	60.4%	63.7%	
<i>Dehydrogenation</i>			
MCH mass flow	147,000	100,000	kg/h
MCH LHV	43.4	43.4	MJ/kg
Toluene mass flow	124150.5	85,298	kg/h
Toluene LHV	40.6	40.6	MJ/kg
Energy required for dehydrogenation	99.9 <sup>b</sup>	– <sup>b</sup>	MW
System Efficiency	22.7% <sup>b</sup>	53.7%	

<sup>a</sup> ASU and O<sub>2</sub> are not required owing to the air-fuel combustion type in the proposed model

<sup>b</sup> The dehydrogenation process for the Graz cycle was calculated based on a stoichiometric reaction, using a conservative heat recovery system.

### 3.3. Overall performance including MCH production (hydrogenation)

MCH production is carried out in hydrogenation plant, where H<sub>2</sub> is bonded with toluene, resulting in the MCH formation. Hydrogenation is an exothermic reaction, producing heat as one of results of reaction. As mentioned above, theoretically, MCH has volumetric and gravimetric hydrogen content of 47% and 6.2%, respectively. Hydrogenation process including the catalyst used in the reaction is considered a well-established technology with the reaction as follow,



The produced heat from hydrogenation reaction can be recovered by other system that is coupled with hydrogenation plant. Aziz and his co-workers have developed and reported several integrated hydrogen production and power generation systems from microalgae [34], low rank coal with syngas chemical looping [11], and brown coal with direct chemical looping [30]. In their developed system, hydrogen which is produced from the system, was bonded with toluene in hydrogenation

plant. The remaining syngas is utilized as fuel gas in the combined cycle power plant to generate electricity. The excess heat produced from hydrogenation reaction is recovered for preheating the cold stream flow of combined cycle, reducing the exergy loss of the system. Therefore, highly efficiency system can be achieved.

Typical condition of hydrogenation process is presented in Table 4. Hydrogenator consist of a mixer, reactor, and heat exchanger. Fixed bed reactor is employed with catalyst loaded inside the bed.

In case of coal as the primary resource for hydrogen production, based on [11,30], the total energy efficiencies, including produced hydrogen which is hydrogenated in MCH and generated power, for each syngas and direct chemical looping are 84% and 91%, respectively. Combining those studies and the obtained result in the current study, the overall energy efficiency from primary energy source (coal) to the generated power at the utilization site after dehydrogenation is about 46–49%. This is considered very high and can be achieved due to effective heat circulation through enhanced process integration.

## 4. Conclusion

An integrated system using dehydrogenation and a power generation process was proposed to gain energy from chemically bonded H<sub>2</sub> in MCH. MCH/toluene has been well reported as a promising H<sub>2</sub> storage system, and has been practically applied at an industrial scale. A highly endothermic dehydrogenation reaction is covered by the heat generated from the air-fuel combustion of H<sub>2</sub>. Moreover, the remaining heat is supplied to the combined cycle plant, and optimized using enhanced process integration (EPI) to reduce the exergy loss, leading to a highly efficient system.

A comparison between the proposed integrated-system and a Graz cycle-based system was carried out to evaluate the overall system performance. The results show that the proposed integrated system can provide energy for the dehydrogenation process while maintaining a highly efficient combined cycle as the power generation system. The power generation efficiency of the proposed integrated system is higher than that of the Graz cycle-based system, mainly owing to the air-fuel combustion, which requires less energy and fewer components. With a higher combustion temperature and heat recovery optimization, the proposed integrated system has a significantly high system efficiency of 53.7%, compared to that of the Graz cycle based-system, at 23%.

## Acknowledgment

This research was supported by JSPS KAKENHI Grant No. 16K18355. F.B.J. acknowledges the Indonesia Endowment Fund for Education (LPDP) for their support of this study.

**Table 4**  
Typical condition of hydrogenation plant.

Parameter	Value	Symbol (Refer to Fig. 2)
Pressure (kPa)	130	–
Temperature (°C)	200	F20
Catalyst	Ni-Mo/Al <sub>2</sub> O <sub>3</sub>	F20
Catalyst particle size (mm)	0.3	–
Sphericity (–)	0.5	–



## References

- [1] International Energy Agency. Executive Summary - Medium-Term Renewable Energy Market Report; 2016.
- [2] M. Bhattacharya, S.R. Paramati, I. Ozturk, S. Bhattacharya, The effect of renewable energy consumption on economic growth: Evidence from top 38 countries, *Appl Energy* 162 (2016) 733–741.
- [3] H. Quan, D. Srinivasan, A.M. Khambadkone, A. Khosravi, A computational framework for uncertainty integration in stochastic unit commitment with intermittent renewable energy sources, *Appl Energy* 152 (2015) 71–82.
- [4] M. Robinus, et al., Power-to-gas: electrolyzers as an alternative to network expansion – an example from a distribution system operator, *Appl Energy* 210 (2018) 182–197, May 2017.
- [5] L. Schlapbach, A. Züttel, Hydrogen-storage materials for mobile applications, *Nature* 414 (6861) (Nov. 2001) 353–358.
- [6] G. Gahleitner, Hydrogen from renewable electricity: An international review of power-to-gas pilot plants for stationary applications, *Int J Hydrogen Energy* 38 (5) (Feb. 2013) 2039–2061.
- [7] I. Dincer, Hydrogen and fuel cell technologies for sustainable future, *JMIE* 2 (1) (2008).
- [8] I.N. Zaini, A. Nurdinawati, M. Aziz, Cogeneration of power and H<sub>2</sub> by steam gasification and syngas chemical looping of macroalgae, *Appl Energy* 207 (2017) 134–145.
- [9] H. Zhang, W. Chen, W. Huang, TIMES modelling of transport sector in China and USA: comparisons from a decarbonization perspective, *Appl Energy* 162 (2016) 1505–1514.
- [10] A. Sarkar, R. Banerjee, Net energy analysis of hydrogen storage options, *Int J Hydrogen Energy* 30 (8) (Jul. 2005) 867–877.
- [11] M. Aziz, F.B. Juangsa, W. Kurniawan, B.A. Budiman, Clean Co-production of H<sub>2</sub> and power from low rank coal, *Energy* 116 (Dec. 2016) 489–497.
- [12] J. Graetz, New approaches to hydrogen storage, *Chem Soc Rev* 38 (1) (Dec. 2009) 73–82.
- [13] M. Bracha, G. Lorenz, A. Patzelt, M. Wanner, Large-scale hydrogen liquefaction in Germany, *Int J Hydrogen Energy* 19 (1) (Jan. 1994) 53–59.
- [14] C.R. Baker, R.L. Shaner, A study of the efficiency of hydrogen liquefaction, *Int J Hydrogen Energy* 3 (3) (1978) 321–334.
- [15] P. Preuster, C. Papp, P. Wasserscheid, Liquid Organic Hydrogen Carriers (LOHCs): toward a hydrogen-free hydrogen economy, *ACC Chem Res* 50 (1) (Jan. 2017) 74–85.
- [16] M. Aziz, A. Putranto, M.K. Biddinika, A.T. Wijayanta, Energy-saving combination of N<sub>2</sub> production, NH<sub>3</sub> synthesis, and power generation, *Int J Hydrogen Energy* 42 (44) (Nov. 2017) 27174–27183.
- [17] N. Brautbar, M.P. Wu, E.D. Richter, Chronic ammonia inhalation and interstitial pulmonary fibrosis: a case report and review of the literature, *Arch. Environ. Heal. An Int. J.* 58 (9) (Sep. 2003) 592–596.
- [18] Okada Y, Shimura M. Development of large-scale H<sub>2</sub> storage and transportation technology with Liquid Organic Hydrogen Carrier (LOHC). *Jt. GCC-JAPAN Environ. Symp.*; 2013.
- [19] M. Aziz, I.N. Zaini, Hydrogen production from algal pathways, in: *Encyclopedia of sustainability science and technology*, Springer New York, New York, NY, 2018, pp. 1–28.
- [20] N. Brückner, et al., Evaluation of industrially applied heat-transfer fluids as liquid organic hydrogen carrier systems, *ChemSusChem* 7 (1) (Jan. 2014) 229–235.
- [21] A. Fikrt, et al., Dynamic power supply by hydrogen bound to a liquid organic hydrogen carrier, *Appl Energy* 194 (May 2017) 1–8.
- [22] G. Li, K. Yada, M. Kanezashi, T. Yoshioka, T. Tsuru, Methylcyclohexane dehydrogenation in catalytic membrane reactors for efficient hydrogen production, *Ind Eng Chem Res* 52 (37) (Sep. 2013) 13325–13332.
- [23] M.D.I. Hatim, M.A.U. Fazara, A.M. Syarhabil, F. Riduwan, Catalytic dehydrogenation of methylcyclohexane (MCH) to toluene in a palladium/alumina hollow fibre membrane reactor, *Procedia Eng.* 53 (Jan. 2013) 71–80.
- [24] G.W.H. Scherer, E. Newson, Analysis of the seasonal energy storage of hydrogen in liquid organic hydrides, *Int J Hydrogen Energy* 23 (1) (1998) 19–25.
- [25] M. Turco, A. Ausiello, L. Micoli, Treatment of biogas for feeding high temperature fuel cells, Springer International Publishing, Cham, 2016.
- [26] Sanz W, Braun M, Jericha H, Platzer MF. Adapting the zero-emission graz cycle for hydrogen combustion and investigation of its part load behaviour. In: *Proceedings of ASME Turbo Expo*; 2016.
- [27] S. Malysenko, A. Gryaznov, N. Filatov, High-pressure H<sub>2</sub>/O<sub>2</sub>-steam generators and their possible applications, *Int J Hydrogen Energy* 29 (6) (May 2004) 589–596.
- [28] J. Milewski, Hydrogen utilization by steam turbine cycles, *J J Power Technol.* 95 (4) (2015) 258–264.
- [29] A. Cappelletti, F. Martelli, V.S. Marta, Investigation of a pure hydrogen fueled gas turbine burner, *Int J Hydrogen Energy* 42 (15) (2017) 10513–10523.
- [30] M. Aziz, I.N. Zaini, T. Oda, A. Morihara, T. Kashiwagi, Energy conservative brown coal conversion to hydrogen and power based on enhanced process integration: Integrated drying, coal direct chemical looping, combined cycle and hydrogenation, *Int J Hydrogen Energy* 42 (5) (Feb. 2017) 2904–2913.
- [31] M. Aziz, T. Oda, T. Kashiwagi, Integration of energy-efficient drying in microalgae utilization based on enhanced process integration, *Energy* 70 (Jun. 2014) 307–316.
- [32] A. Darmawan, F. Hardi, K. Yoshikawa, M. Aziz, K. Tokimatsu, Enhanced process integration of black liquor evaporation, gasification, and combined cycle, *Appl Energy* 204 (2017) 1035–1042.
- [33] M. Aziz, Y. Kansha, A. Kishimoto, Y. Kotani, Y. Liu, A. Tsutsumi, Advanced energy saving in low rank coal drying based on self-heat recuperation technology, *Fuel Process Technol* 104 (Dec. 2012) 16–22.
- [34] M. Aziz, Integrated hydrogen production and power generation from microalgae, *Int J Hydrogen Energy* 41 (1) (Jan. 2016) 104–112.
- [35] B. Prabowo, M. Aziz, K. Umeki, H. Susanto, M. Yan, K. Yoshikawa, CO<sub>2</sub>-recycling biomass gasification system for highly efficient and carbon-negative power generation, *Appl Energy* 158 (Nov. 2015) 97–106.
- [36] J. Sug Lee, K. Ogawa, Pressure drop though packed bed, *J Chem Eng Jpn* 24 (5) (1994) 691–693.
- [37] M. Usman, D. Cresswell, A. Garforth, Detailed reaction kinetics for the dehydrogenation of methylcyclohexane over Pt catalyst, *Ind Eng Chem Res* 51 (1) (Jan. 2012) 158–170.
- [38] Alhumaidan F, Cresswell D, Garforth A. Hydrogen storage in liquid organic hydride: producing hydrogen catalytically from methylcyclohexane. *Energy and Fuels* 25(10). American Chemical Society. p. 4217–4234, 20-Oct-2011.
- [39] F. Alhumaidan, D. Tsakiris, D. Cresswell, A. Garforth, Hydrogen storage in liquid organic hydride: Selectivity of MCH dehydrogenation over monometallic and bimetallic Pt catalysts, *Int J Hydrogen Energy* 38 (32) (Oct. 2013) 14010–14026.
- [40] Sanz W, Jericha H, Moser M, Heitmeir F. Thermodynamic and economic investigation of an improved graz cycle power plant for CO. In: *Volume 7: Turbo Expo 2004, 2004*, p. 409–18.
- [41] T.K. Ibrahim, M.M. Rahman, Effect of compression ratio on performance of combined cycle gas turbine, *Int J Energy Eng* 2 (1) (Aug. 2012) 9–14.
- [42] C.-C. Chuang, D.-C. Sue, Performance effects of combined cycle power plant with variable condenser pressure and loading, *Energy* 30 (10) (Jul. 2005) 1793–1801.

# HASIL CEK\_Highly energy-efficient combination of dehydrogenation of methylcyclohexane and hydrogen-based power generation

## ORIGINALITY REPORT

5%

SIMILARITY INDEX

5%

INTERNET SOURCES

7%

PUBLICATIONS

0%

STUDENT PAPERS

## PRIMARY SOURCES

1

[www.cheric.org](http://www.cheric.org)  
Internet Source

5%

Exclude quotes On

Exclude bibliography On

Exclude matches < 2%